Tunable molecular editing of indoles with fluoroalkyl carbenes

Shaopeng Liu
Northeast Normal University https://orcid.org/0000-0002-9509-4542
Yong Yang
Northeast Normal University https://orcid.org/0000-0002-8523-3879
Qingmin Song
Northeast Normal University https://orcid.org/0000-0003-3546-2961
Zhaohong Liu
Northeast Normal University https://orcid.org/0000-0001-9951-8675
Ying Lu
Northeast Normal University https://orcid.org/0000-0001-7152-7617
Zhanjing Wang
Northeast Normal University https://orcid.org/0000-0001-6687-5991
Paramasivam Sivaguru
Northeast Normal University https://orcid.org/0000-0003-2225-0054
Xihe Bi
bixh507@nenu.edu.cn
Northeast Normal University https://orcid.org/0000-0002-6694-6742

Article

Keywords:

Posted Date: February 22nd, 2023

DOI: https://doi.org/10.21203/rs.3.rs-2466531/v1

Additional Declarations: There is **NO** Competing Interest.

Version of Record: A version of this preprint was published at Nature Chemistry on March 5th, 2024. See the published version at https://doi.org/10.1038/s41557-024-01468-2.

Abstract

Building molecular complexity from simple feedstocks through peripheral and skeletal editing is central to modern organic synthesis. Nevertheless, a controllable strategy that can modify both the core skeleton and periphery of an aromatic heterocycle with a common substrate remains undeveloped, despite its potential to maximize structural diversity and applications. Here we report a fluoroalkyl carbene-initiated chemodivergent molecular editing of indoles, allowing both skeletal and peripheral editing by trapping electrophilic fluoroalkyl carbene generated *in situ* from fluoroalkyl *N*-triftosylhydrazones. A variety of fluorine-containing *N*-heterocyclic scaffolds could be efficiently achieved through the tunable chemoselective editing reactions at skeleton or periphery of the indole, including one-carbon insertion, C3−H *gem*-difluoroolefination, tandem cyclopropanation/N1−H *gem*-difluoroolefination, and cyclopropanation. Mechanistic experiments and computations have probed the reaction mechanism and the origins of chemo- and regioselectivity.

One-Sentence Summary

Chemodivergent skeletal and peripheral editing of indoles was achieved using fluoroalkyl *N*-triftosylhydrazone as a common editing reagent.

Introduction

"Molecular editing" reactions have revolutionized modern organic synthesis because it allows the rapid transition of simple substrates into uncharted chemical space, including the development of drug candidates (*1*–*3*). Given the ubiquity of C − H bonds in molecules, C − H functionalization (peripheral editing) is the most flexible and universal molecular editing strategy for adding complexity to a starting molecule (*4*–*11*). On the other hand, skeletal editing – the process by which single atoms can be inserted (*12*–*14*) or deleted (*15*–*19*), or transmuted (*20*) in or around the molecular skeleton is conceptually new and transformative to synthetic chemists (Fig. 1A). The retrosynthetic simplicity of single-atom skeletal editing has recently aroused increasing interest in the streamlined development of new drugs via late-stage functionalization (*1*–*3*). Despite significant progress with saturated heterocycles (*2*), the stability of aromatic systems makes skeletal editing of heteroaromatics poses a significant challenge (*21*). As one of the most abundant aromatic *N*-heterocycles and the privileged pharmacophores (*22*–*27*), indoles represent an ideal target for molecular editing. Recent advancements in indole molecular editing have been focused on dearomative cyclization (*23*–*25*) or C − H functionalization (*26,27*), allowing the construction of diverse fused *N*-heterocycles or the installation of a variety of useful functional groups onto the indole core, such as silyl (*28*), boryl (2*9,30*), alkyl (*31*), allyl (*32*), alkenyl (*33*), alkynyl (*34*), and aryl groups (*35*). In sharp contrast, only a few reports have demonstrated the more challenging but exciting skeletal editing of indoles involving the cleavage of inert aromatic C = C bonds in complex settings (*36,37*). As one of the pioneers in single-atom skeletal editing, Levin and coworkers reported a chlorodiazirine-promoted carbon-atom insertion into indoles to obtain 3-arylquinoline motifs (*36*). The Morandi group achieved skeletal editing of indoles via nitrogen atom insertion affording quinazolines,

where silyl-protected indole and iodonitrene reagent were required (*37*). Despite these impressive advances, existing peripheral and skeletal editings typically rely on different strategies and starting materials, curtailing broader translational realization. Hence, we envisioned that the ability to switchable editing both the core skeleton and the periphery with a common editing reagent could expedite the omnidirectional exploration of chemical space around lead compounds, greatly facilitating drug discovery (Fig. 1B).

Strategically introducing a fluorinated group, such as trifluoromethyl (CF_3) and *gem*-difluorovinyl, into aromatic *N*-heterocycles can profoundly alter their physical and pharmacokinetic properties (*38*), resulting in a plethora of listed drugs (Fig. 1C) (*39,40*). The most widely utilized way to achieve these targets includes the metal-catalyzed cross-couplings of a fluorination reagent to the prefunctionalized substrate (*41*,*42*) and direct C − H functionalization reactions (*43–46*). Although trifluoromethylated quaternary stereocenters are one of the most common structural motifs in lead compounds and marketed drugs (*36*), the direct insertion of a fluoroalkyl group into the indole skeleton to construct medicinally interesting fluorinated structures remains challenging and virtually unknown (*47,48*). Herein, we report a strategically distinct molecular editing reaction that enables both skeletal and peripheral indoles editing by trapping electrophilic fluoroalkyl carbenes generated *in situ* from fluoroalkyl *N*-triftosylhydrazones (*48,49*) in a tunable manner (Fig. 1D). Various peripheral molecular editing reactions of indoles, including C3 − H *gem*-difluoroolefination, cyclopropanation, and tandem cyclopropanation/N1 − H *gem*-difluoroolefination, as well as a challenging skeletal editing by one-carbon insertion into aromatic C = C bonds, all successfully achieved with excellent chemo- and regiocontrol by varying the reaction conditions. These divergent transformations provide direct access to quinoline- and indole-based bicyclic compounds with bioisosteric trifluoromethyl or *gem*-difluorovinyl groups, which are not so common in medicinal chemistry libraries but are widely acknowledged as privileged pharmacophores in modern drug discovery (*39,40*). This ideal molecular editing strategy thus paves the way for the construction of drug candidate libraries by selectively modifying their core structure and the periphery with common editing reagents and tunable catalytic conditions.

Results And Discussion

To achieve chemodivergent molecular editing of *N*-unprotected indoles with fluoroalkyl carbenes, the site- and chemoselectivity control issues between the relatively low reactive C3 − H bond and innate reactivity of nucleophilic nitrogen atom resulting in a mixture of C2-, C3-, and/or N1-functionalization and cyclopropanation products must be overcome (Fig. 2A) (*50*, *51*). We began by concentrating on the development of a selective skeletal editing reaction (see Table S1 for details). The initial reaction of 5-bromo-1*H*-indole (**1**, 2.0 equiv) and trifluoromethyl phenyl *N*-triftosylhydrazone (**2**, 1.0 equiv) with $Rh_2(OAc)_4$ and NaH in trifluorotoluene at 60°C produced the carbon insertion product, 3,4-dihydroquinoline (**3**) in 52% yield, along with C3 − H *gem*-difluorination product (**4**) in 10% yield (entry 1, Fig. 2B). The structure of **3** was explicitly confirmed by X-ray crystallography. Further optimizations reveal that Tp^{Br3}Ag(thf) was the most effective, delivering the desired carbon insertion product (**4**) in 96%

isolated yield with three equivalents of **1** at 80°C (entry 3). Changing the ratio of **1** and **2** from 3:1 to 1:3 shut down the skeletal editing pathway while providing a 90% yield of the peripheral (i.e., a tandem cyclopropanation and N1 − H *gem*-difluoroolefination) functionalization product **5** (entry 4). The product yield was increased to 98% by running the reaction in DCE (1,2-dichloroethane) at 60°C (entry 5). Switching the NaH base with *N*,*N*-diisopropylethylamine (DIPEA) led to the selective C3 − H *gem*-difluoroolefination, producing product **4** in 40% yield (entry 6). A systematic survey of reaction parameters disclosed that the reaction of **1** (1.0 equiv) and **2** (2.0 equiv) with the $Rh_2(OAc)_4$/DIPEA catalytic system in trifluorotoluene at 25°C improved the product yield to 92% (entry 8). In this way, we were able to perform C3 − H *gem*-difluoroolefination of *N*-unprotected and *N*-aryl indoles, which was not possible by Koenigs palladium-catalyzed reaction using diazoalkanes as carbene precursors (*52*).

Using these optimized conditions, the substrate scope of the carbon insertion reaction was then investigated (Fig. 3A). Trifluoromethyl phenyl *N*-triftosylhydrazones featuring electron-donating (e.g., methyl, *tert*-butyl, methoxy, trifluoromethoxy), electron-withdrawing (e.g., trifluoromethyl, ester, vinyl, and nitro), and electon-nutral (e.g., phenyl and halogens) groups provided good to excellent yields of carbon insertion products (**6**–**24**). The presence of *o*-substituents (**18**–**21**) and a 3-nitro substituent (**24**) on the phenyl ring of *N*-triftosylhydrazone resulted in lower yields, likely due to increased steric hindrance. The disubstituted phenyl substrates were also well tolerated (**25** and **26**). 3,4-Dihydroquinoline products containing naphthyl (**29**) and heterocycles such as 1,3-benzodioxole (**27**), 2,3-dihydrobenzo[*b*][1,4]dioxine (**28**), furan (**31**), thiophene (**32**), dibenzothiophene (**30**), benzothiophene (**33**), and *N*-methyl indole (**34**), were obtained in moderate to good yields from the corresponding *N*-triftosylhydrazones. We also noticed that trifluoromethyl alkyl *N*-triftosylhydrazones reacted smoothly (**35** and **36**), albeit with lower yields due to competitive self-coupling of fluoroalkyl carbene. This carbon insertion methodology was also extended to electron-poor (e.g., esters, halogens, phenyl, formyl, acetyl, tosylate, and nitrile) and electron-rich (e.g., ethers, methyl, and *tert*-butyldimethylsilyl ethers) indoles and obtained the desired 3,4-dihydroquinoline products (**37**–**54**, **57**) in moderate to good yields. Here, the reaction was shown to be sensitive to the position of substituents, with 4-substituted indoles giving lower yields than 5- or 6- or 7-substituted indoles. Indoles with an unsaturated unit performed well in the skeletal ring expansion chemistry, providing an additional functional handle for post-ring expansion functionalizations (**55** and **56**). Disubstituted indoles also proved to be suitable (**58**–**60**). Finally, we applied this skeletal ring expansion strategy in a one-pot, two-step reaction. Using commercially available indoles as starting materials, a tandem carbon insertion and reduction (with $NaBH_4$) resulted in high yields of the corresponding tetrahydroquinoline products (**61**–**63**) without the isolation of intermediates (Fig. 3B).

The skeletal ring expansion of indoles could be scalable. The carbon insertion reaction on a 5 mmol scale of **2** with 5-bromoindole could still provide the corresponding 3,4-dihydroquinoline product **3** in good yield (1.4 g, 80%). The simple transformations of **3** could yield a variety of synthetically useful scaffolds, amplifying the synthetic utility of product **3** (Fig. 3C). Grignard reactions on the N = C bond in product **3** results in corresponding 2-arylated-, 2-allylated-, and 2-alkylated tetrahydroquinoline products (**64–66**) in high yields and good diastereomeric ratio (d.r.). Subjecting compound **3** to PINNICK oxidation conditions

yielded the 3,4-dihydroquinolin-2(1*H*)-one (**67**). The bromo group in product **3** could undergo a variety of cross-coupling reactions. For example, the Buchwald-Hartwig cross-coupling of **3** with aniline furnished the desired *N*-phenyl-3,4-dihydroquinoline-6-amine (**68**), whereas the copper-catalyzed amination with aqueous ammonia yielded 6-amino-3,4-dihydroquinoline (**69**). This amino compound class is an important building block in pharmacology and materials science. The Suzuki-Miyaura coupling of **3** with benzofuran-2-boronic acid produced 6-(benzofuran-2-yl)-3,4-dihydroquinoline (**70**).

Next, we examined the scope and limitations of the developed methodology in C3 − H *gem*-difluoroolefination of indoles (Fig. 4A). An array of trifluoromethyl aryl *N*-triftosylhydrazones with various functional handles reacted well with *N*-unprotected indoles, affording the corresponding products (**71**–**80**) in moderate to good yields. Substrates containing disubstituted phenyl, naphthyl, and heterocyclic frameworks exclusively afforded the corresponding products (**81**–**85**) in good yields. *N*-Unprotected indoles with diverse substituents (e.g., methyl, fluoro, bromo, chloro, and cyano) on any of the positions were also successfully converted to the desired *gem*-difluoroolefination products (**86**–**94**). When compared to methyl and halogen groups, electron-withdrawing (e.g., fluoro and cyano) groups on indoles resulted in slightly lower yields of products (**91** and **94**). The α-C − F bond was predominantly activated when using *N*-triftosylhydrazone derived from pentafluoroethyl phenyl ketone, leading to **95** (78% yield), as confirmed by single-crystal X-ray analysis.

The applicability of this protocol with various *N*-substituted indoles was then assessed. Under the optimized conditions, a variety of aryl, naphthyl, alkyl, benzyl, propargyl, and allyl-protected indoles were also suitable substrates, affording the desired products (**96**–**121**) in good to excellent yields. The unsaturated group in the substrates remained intact, demonstrating the chemoselectivity of the process. *N*-Triftosylhydrazones derived from alkyl trifluoromethyl ketones could also be used as substrates, although low yields were observed (**122** and **123**). This transformation was compatible with a variety of functional groups. These *gem*-difluoroolefin products were difficult to obtain by existing methods (*47*).

Having established the optimal conditions for chemoselective assembling of N1-*gem*-difluorovinyl tetrahydrocyclopropa[*b*]indoles, we sought to apply the developed protocol to other substrates (Fig. 4B). Trifluoromethyl phenyl *N*-triftosylhydrazones with substituents on the 4-position (e.g., halogens, vinyl, trifluoromethyl, trifluoromethoxy) and a 3,5-dimethoxy substituted substrate reacted in moderate to good yields (**124**–**130**). Substrates derived from polycyclic rings such as naphthyl- and 2,3-dihydrobenzo[*b*][1,4]dioxine were found to be compatible in this reaction (**141** and **138**), paving the way for late-stage diversification of complex molecules. The tolerance of various functional groups on the indole core was then examined. Regardless of positions and electronic effects, indoles with methoxy, esters, and iodo groups underwent this tandem reaction to afford the corresponding products in high yields (**132**–**136**). The 5-fluoro-6-bromo indole was also smoothly transformed to the desired products **137** in 84% yield.

Finally, we pursued the development of a dearomative cyclopropanation reaction (*44*–*46*). After the systematic screening of reaction conditions, the subjection of *N*-methylindole (2.0 equiv) with **2** (1.0 equiv) in trifluorotoluene at 60°C in the presence of NaH and $Rh_2(OAc)_4$ afforded the corresponding

cyclopropane (**139**) in 97% yield (Fig. 4C, See Table S2 for details). Applying the optimized conditions, we investigated the substrate scope of this dearomative cyclopropanation. As shown in Fig. 4C, a series of trifluoromethyl aryl *N*-triftosylhydrazones successfully participated in this reaction with *N*-methyl indole, affording *N*-methyl-tetrahydrocyclopropa[*b*]indoles (**140**–**143**) in high yields. Similarly, the *N*-triftosylhydrazones derived from disubstituted phenyl-, naphthyl-, piperonyl-, fluorenyl-, and furyl trifluoromethyl ketone were cyclopropanated (**144**–**149**). Both electron-donating (e.g., methyl) and electron-withdrawing (e.g., halogens, cyano, ester) groups on *N*-methyl indoles were compatible in the reaction (**150**–**154**). The little difference in yield confirms the effectiveness of our method in overriding inherent electronic preferences. *N*-Hexyl and *N*-benzyl indoles were also converted smoothly into corresponding cycloadducts **155** and **156** in 91% and 60% yield, respectively. The transformation was not limited to *N*-alkyl indoles; a variety of *N*-aryl indoles with various functionalities, *N*-naphthyl-, and *N*-pyrimidinyl indoles also performed well in this reaction (**157**–**164**). The identity of **163** was further confirmed by X-ray analysis. Other functional groups such as acetyl-, pivaloyl-, carbamoyl-, tosyl-, and TBS-protected indoles were found effective in producing tetrahydrocyclopropa[*b*]indole products (**165**–**169**). *N*-Triftosylhydrazone derived from pentafluoroethyl phenyl ketone was also a competent substrate, furnishing the corresponding product (**170**) in 83% yields.

The gram-scale synthesis of **108** (1.3 g, 96% yield) via C3-H *gem*-difluoroolefination also proceeded smoothly, demonstrating the scalability of the process (Fig. 5A). To demonstrate the synthetic utility of *gem*-difluoroalkenyl group, we performed a cyclization reaction between **108** and benzoyl hydrazine in the presence of Cs_2CO_3, which afforded an unsymmetrical 2,5-disubstituted 1,3,4-oxadiazoles (**171**) in 61% yield. Given the importance of trifluoromethyl and *gem*-difluorides in medicinal chemistry, the late-stage skeletal and peripheral editing of indole alkaloids could benefit the discovery of new drug analogous (Fig. 5B). Subjecting excess of Verticillatine B and Raputimonoindole B, two bioactive compounds isolated from neotropical plants, to our optimized Tp^{Br3}Ag/NaH catalytic system generated the corresponding carbon insertion products **172** and **175**, respectively, whereas the C3-*gem*-difluoroolefination products **173** and **176** were isolated using $Rh_2(OAc)_4$/DIPEA catalytic system. Treatment of Verticillatine B and Raputimonoindole B with excess *N*-triftosylhydrazones **2** provided the tandem cyclopropanation and N1-*gem*-difluoroolefination products **174** and **177** under the Tp^{Br3}Ag/NaH catalytic system.

Mechanistic Investigations

To understand the origin of chemoselectivity, a series of control experiments were conducted using phenyl trifluoromethyldiazomethane as a carbene precursor (Fig. 6B). These results suggest that the chemoselectivity of the reaction is dependent on the base (NaH or DIPEA) used and the ratio of silver carbene and indole (Fig. 6B). No N1 – H functionalization was observed in all cases, which differs fundamentally from previously reported reactions of *N*-unprotected indoles with metal carbenes (*44*, *45*). To gain deeper insight into the reaction mechanism and the origin of this unusual chemoselectivity, we performed density functional theory (DFT) calculations at the SMD(DCM)//B3LYP-GD3(BJ)/6–31 +

G(d,p)-SDD(Ag, Br or Rh) level of theory (For details see Figs. S1 to S6). As shown in Fig. 6A, electrophilic metal carbene preferentially attacks the more nucleophilic C3 position of indole **178** to produce **IntII-Ag** and **IntII-Rh**. The calculated energy for **TSI-Ag** to **IntII-Ag** was 4.0 kcal mol^{-1} lower than that for **TSI-Ag'**, resulting in unfavourable **N1 – H** functionalization (Fig. 6D). Fukui function analysis (*53*, *54*) was also performed on **TSI-Ag** and **TSI-Ag'**, which support the hypothesis that the indole C3 position is more nucleophilic than the N1 position (Fig. 6E).

When using DIPEA as the base, $DIPEAH^+$-assisted β-F elimination of **IntII-Rh** preferentially occurred, where the hydrogen bonding (C – H···F and N – H···F in **TSIII-Rh**) between the DIPEA and CF_3 group playing a dual role in lowering the energy barrier of β-F elimination process and assisting deprotonation to form C3-*gem*-difluoroolefination product **179**. The lack of such hydrogen-bonding effect with the $Tp^{Br3}Ag$/NaH catalytic system favours 2,3-cyclopropanation of **IntII-Ag** over β-F elimination (Fig. 6C). In the presence of excessive indoles, the cyclopropane intermediate **IntIII** undergoes a tandem rate-determining hydrogen atom abstraction by NaH ($\Delta G^{\neq}$ = 12.3 kcal mol^{-1}), reversible ring opening ($\Delta G^{\neq}$ = 12.1 kcal mol^{-1}), and water-assisted protonation ($\Delta G^{\neq}$ = 3.0 kcal mol^{-1}) to give the carbon insertion product **181** (Fig. 6A). When silver carbene **IntI-Ag** is excessive, the nucleophilic attack of **IntIII** on silver carbene **IntI-Ag** via **TSIII-Ag'** occurs to form kinetically favourable ylide **IntIV'**, which then undergo β-F elimination to give N1-*gem*-difluoroolefination product **180** (for details see Fig. S4). The calculated energy for **TSIII-Ag'** is 0.6 kcal mol^{-1} higher than that of **TSI-Ag** (Fig. 6D) and 10.4 kcal mol^{-1} lower than that of **TSIII-Ag**. These observations are consistent with the experimental results that using an excess of indoles affords carbon-atom insertion product **181**, and vice versa.

Conclusion

In summary, chemodivergent skeletal and peripheral editing of indoles was demonstrated using fluoroalkyl carbenes. The reaction relies on the facile *in situ* generation of an electrophilic fluoroalkyl carbene intermediate from fluoroalkyl *N*-triftosylhydrazones, leading to a variety of fluorinated *N*-heterocyclic frameworks with high efficiency and good functional group tolerance. Our experimental and computational findings supported that the combination of an appropriate metal catalysts and a base is critical to the success of the developed molecular editing reactions. Given the abundance of indole cores in bioactive molecules and natural products, this method could be used to simplify the synthesis of complex target molecules by minimizing functional group manipulations or protecting group usages. Taken together, an efficient fluoroalkyl carbene strategy for the tunable editing of heteroaromatics has been demonstrated and would spark more idea in this exciting area.

Declarations

Acknowledgments

Funding: Research reported in this publication was supported by NSFC (21871043, 1961130376), the Department of Science and Technology of Jilin Province (20180101185JC, 20190701012GH,

20200801065GH), and the Fundamental Research Funds for the Central Universities (2412019ZD001, 2412020ZD003).

Author contributions: S.L., Y.Y., and Q.S. contributed equally to this work. S.L., Y.Y., Y.L. and Z.W. performed the experimental investigations and Q.S. carried out the theoretical calculations. Z.L. and X.B. conceived the concept, designed the project, analyzed the data, and together with P.S. discussed the results and prepared this manuscript.

Competing interests: Authors declare that they have no competing interests.

Data and materials availability: Crystallographic data for compound **3**, **64**, **95**, **163** is available free of charge from the Cambridge Crystallographic Data Centre under reference CCDC 2223703, CCDC 2220789, CCDC 2152123, and CCDC 2194938. All other data are available in the main text or the supplementary materials.

References and Notes

1. K. R. Campos *et al*., *Science* **363**, eaat0805 (2019).
2. J. Jurczyk *et al*., *Nat. Synth.* **1**, 352–364 (2022).
3. A. M. Szpilman, E. M. Carreira, *Angew. Chem. Int. Ed.* **49**, 9592–9628 (2010).
4. H. M. L. Davies, K. Liao, *Nat. Rev. Chem.* **3**, 347–360 (2019).
5. L. Guillemard, N. Kaplaneris, L. Ackermann, M. J. Johansson, *Nat. Rev. Chem.* **5**, 522–545 (2021).
6. M. M. Díaz-Requejo, P. J. Peréz, *Chem. Rev.* **108**, 3379-3394 (2008).
7. K. Liao, S. Negretti, D. G. Musaev, J. Bacsa, H. M. L. Davies, *Nature* **533**, 230–234 (2016).
8. K. Liao, T. C. Pickel, V. Boyarskikh, J. Bacsa, D. G. Musaev, H. M. L. Davies, *Nature* **551**, 609–613 (2017).
9. A. Caballero *et al*, *Science* **332**, 835-838 (2011).
10. J. Wencel-Delord, F. Glorius, *Nat. Chem.* **5**, 369–375 (2013).
11. M.-L. Li, J.-H. Yu, Y.-H. Li, S.-F. Zhu, Q.-L. Zhou, *Science* **366**, 990–994 (2019).
12. H. Lyu, I. Kevlishvili, X. Yu, P. Liu, G. Dong, *Science* **372**, 175–182 (2021).
13. E. E. Hyland, P. Q. Kelly, A. M. McKillop, B. D. Dherange, M. D. Levin, *J. Am. Chem. Soc.* **144**, 19258–19264 (2022).
14. S. Liu, X. Cheng, *Nat. Commun.* **13**, 425 (2022).
15. J. Woo *et al*., *Science* **376**, 527–532 (2022).
16. J. Jurczyk *et al*., *Science* **373**, 1004–1012 (2021).
17. S. H. Kennedy, B. D. Dherange, K. J. Berger, M. D. Levin, *Nature* **593**, 223–227 (2021).
18. Z.-C. Cao, Z.-J. Shi, *J. Am. Chem. Soc.* **139**, 6546–6549 (2017)
19. G. L. Bartholomew, F. Carpaneto, R. Sarpong, *J. Am. Chem. Soc.* **144**, 22309–22315 (2022).

20. S. C. Patel, N. Z. Burns, *J. Am. Chem. Soc.* **144**, 17797–17802 (2022).
21. A. Sattler, G. Parkin, *Nature* **463**, 523–526 (2010).
22. X.-Y. Liu, Y. Qin, *Acc. Chem. Res.* **52**, 1877–1891 (2019).
23. Y.-C. Zhang, F. Jiang, F. Shi, *Acc. Chem. Res.* **53**, 425–446 (2020).
24. M. Zhu, X. Zhang, C. Zheng, S.-L. You, *Acc. Chem. Res.* **55**, 2510–2525 (2022).
25. H. Xu *et al.*, *J. Am. Chem. Soc.* **139**, 7697–7700 (2017).
26. J. Wen, Z. Shi, *Acc. Chem. Res.* **54**, 1723–1736 (2021).
27. B. Prabagar, Y. Yang, Z. Shi, *Chem. Soc. Rev.* **50**, 11249–11269 (2021).
28. A. A. Toutov *et al.*, *Nature* **518**, 80–84 (2015).
29. J. Lv *et al.*, *Nature* **575**, 336–340 (2019).
30. M.-A. Légaré, M.-A. Courtemanche, É. Rochette, F.-G. Fontaine, *Science* **349**, 513–516 (2015).
31. Y. Liang, X. Zhang, D. W. C. MacMillan, *Nature* **559**, 83–88 (2018).
32. R, Jiang, L. Ding, C. Zheng, S.-L. You, *Science* **371**, 380–386 (2021).
33. I. Choi, A. M. Messinis, L. Ackermann, *Angew. Chem. Int. Ed.* **59**, 12534–12540 (2020).
34. Z. Ruan, N. Sauermann, E. Manoni, L. Ackermann, *Angew. Chem. Int. Ed.* **56**, 3172–3176 (2017).
35. L.-W. Qi, J.-H. Mao, J. Zhang, B. Tan, *Nat. Chem.* **10**, 58–64 (2018).
36. B. D. Dherange, P. Q. Kelly, J. P. Liles, M. S. Sigman, M. D. Levin, *J. Am. Chem. Soc.* **143**, 11337–11344 (2021).
37. J. C. Reisenbauer, O. Green, A. Franchino, P. Finkelstein, B. Morandi, *Science* **377**, 1104–1109 (2022).
38. K. Müller, C. Faeh, F. Diederich, *Science* **317**, 1881–1886 (2007).
39. Y. Zhu *et al.*, *Chem. Rev.* **118**, 3887–3964 (2018).
40. Y. Zhou *et al.*, *Chem. Rev.* **116**, 422–518 (2016).
41. Y.-J. Yu, *Science* **371**, 1232–1240 (2021).
42. O. A. Tomashenko, V. V. Grushin, *Chem. Rev.* **111**, 4475–4521 (2011).
43. T. Furuya, A. S. Kamlet, T. Ritter, *Nature* **473**, 470–477 (2011).
44. X. Zhang *et al.*, *Nature* **594**, 217–222 (2021).
45. X.-P. Fu *et al.*, *Nat. Chem.* **11**, 948–956 (2019).
46. Z. Feng, Q.-Q. Min, X.-P. Fu, L. An, X. Zhang, *Nat. Chem.* **9**, 918-923 (2017).
47. P. K. Mykhailiuk, *Chem. Rev.* **120**, 12718–12755 (2020).
48. Z. Liu, P. Sivaguru, G. Zanoni, X. Bi, *Acc. Chem. Res.* **55**, 1763–1781 (2022).
49. P. Sivaguru, X. Bi, *Sci. China Chem.* **64**, 1614–1629 (2021).
50. V. Arredondo, S. C. Hiew, E. S. Gutman, I. D. U. A. Premachandra, D. L. V. Vranken, *Angew. Chem. Int. Ed.* **56**, 4156–4159 (2017).
51. M. Delgado-Rebollo, A. Prieto, P. J. Pérez, *ChemCatChem* **6**, 2047–2052 (2014).
52. Z. Yang, M. Möller, R. M. Koenigs, *Angew. Chem. Int. Ed.* **59**, 5572–5576 (2020).

53. W. Yang, R. G. Parr, *Proc. Nati. Acad. Sci.* **82**, 6723–6726 (1985).

54. T. Lu, F. Chen, *J. Comput. Chem.* **33**, 580–592 (2012).

Figures

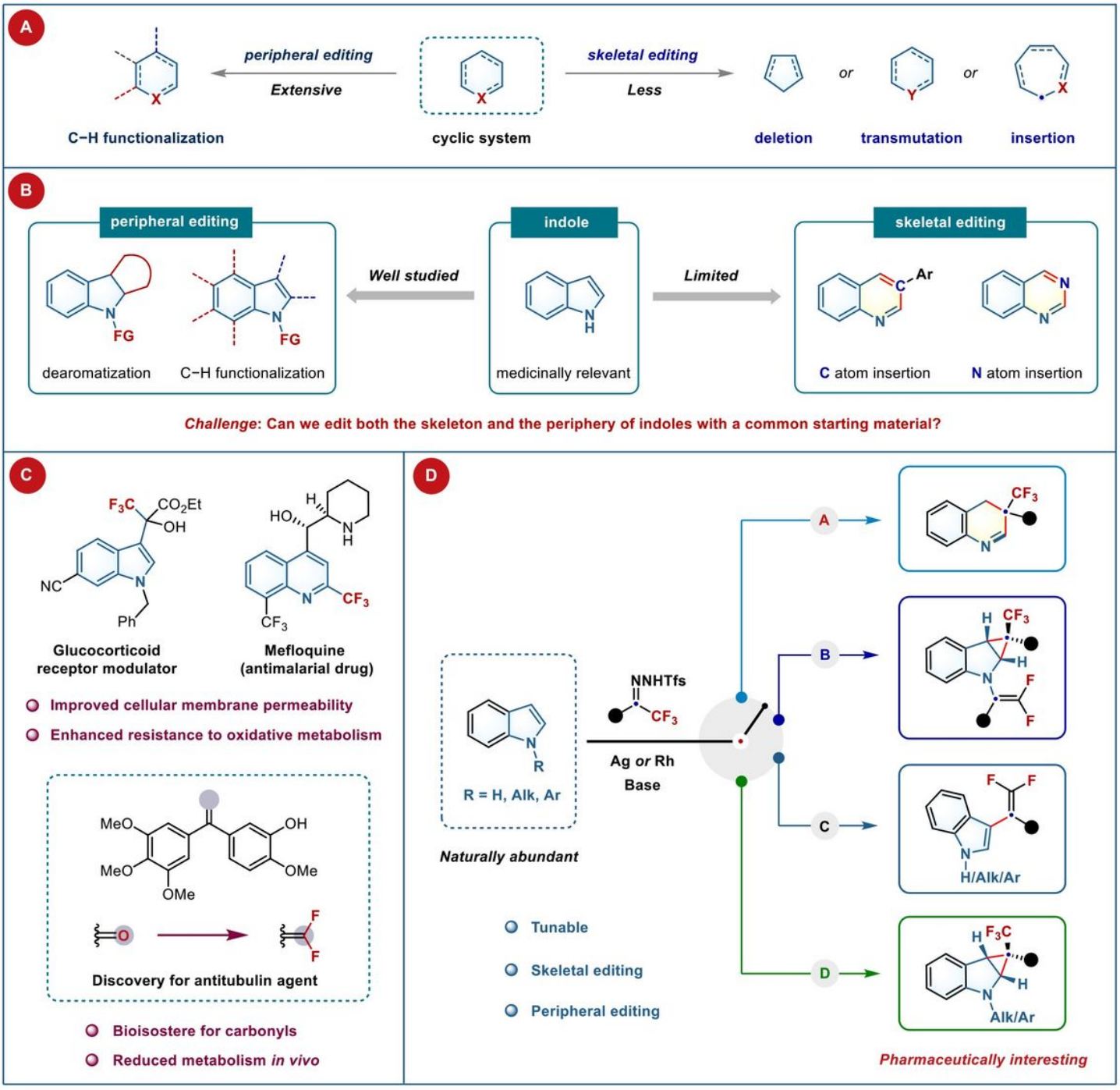

Figure 1

Molecular editing of heterocycles. (**A**) Conceptual outline for peripheral and skeletal editing of heteroaromatics. (**B**) Indoles diversification via peripheral and skeletal editing using different reagents.

(**C**) Representative drugs demonstrate the importance of installing trifluoromethyl and difluoroalkenyl groups into heterocyclic compounds. (**D**) Controllable skeletal and peripheral editing of indoles using fluoroalkyl carbene (this work).

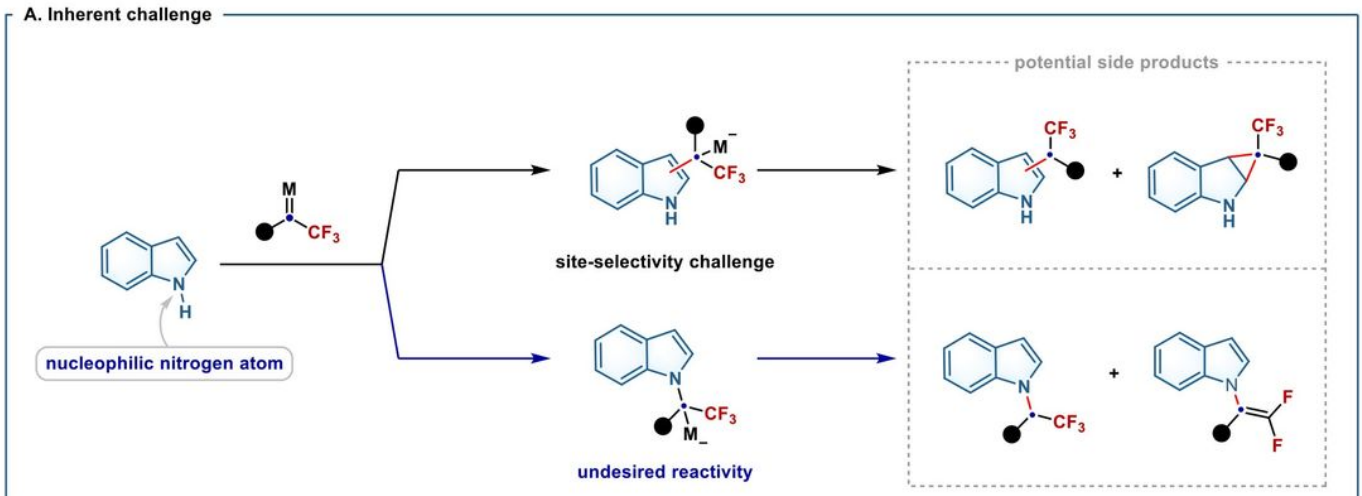

Entry	1:2 ratio	*Cat.* M (x mol%)	Base (y equiv.)	*T* (°C)	3 yield (%)*	4 yield (%)*	5 yield (%)*
1	2:1	$Rh_2(OAc)_4$ (1)	NaH (2)	60	52	10	n.d.
2	2:1	$Tp^{Br3}Ag$(thf) (10)	NaH (2)	60	77	n.d.	n.d.
3	3:1	$Tp^{Br3}Ag$(thf) (10)	NaH (3)	80	**96**	n.d.	n.d.
4	1:3	$Tp^{Br3}Ag$(thf) (10)	NaH (6)	80	trace	n.d.	90
5	1:3	$Tp^{Br3}Ag$(thf) (10)	NaH (6)	60	trace	n.d.	**98**¶
6	1:3	$Tp^{Br3}Ag$(thf) (10)	DIPEA (6)	60	n.d.	40	n.d.
7	1:2	$Tp^{Br3}Ag$(thf) (10)	DIPEA (6)	25	n.d.	60	10
8	1:2	$Rh_2(OAc)_4$ (1)	DIPEA (6)	25	n.d.	**92**	trace
9	1:2	$Rh_2(esp)_2$ (1)	DIPEA (6)	25	n.d.	88	5

Figure 2

Reaction development. (**A**) Inherent challenges for electrophilic metallocarbene insertion into *N*-unprotected indole scaffold. (**B**) Optimization of molecular editing of *N*-unprotected indoles with

fluoroalkyl carbenes. Reactions were performed on a 0.3 mmol scale. †Phenyl(trifluoromethyl) diazomethane as the carbene precursor. *Yield of the isolated product. ¶1,2-Dichloroethane (DCE) as the solvent.

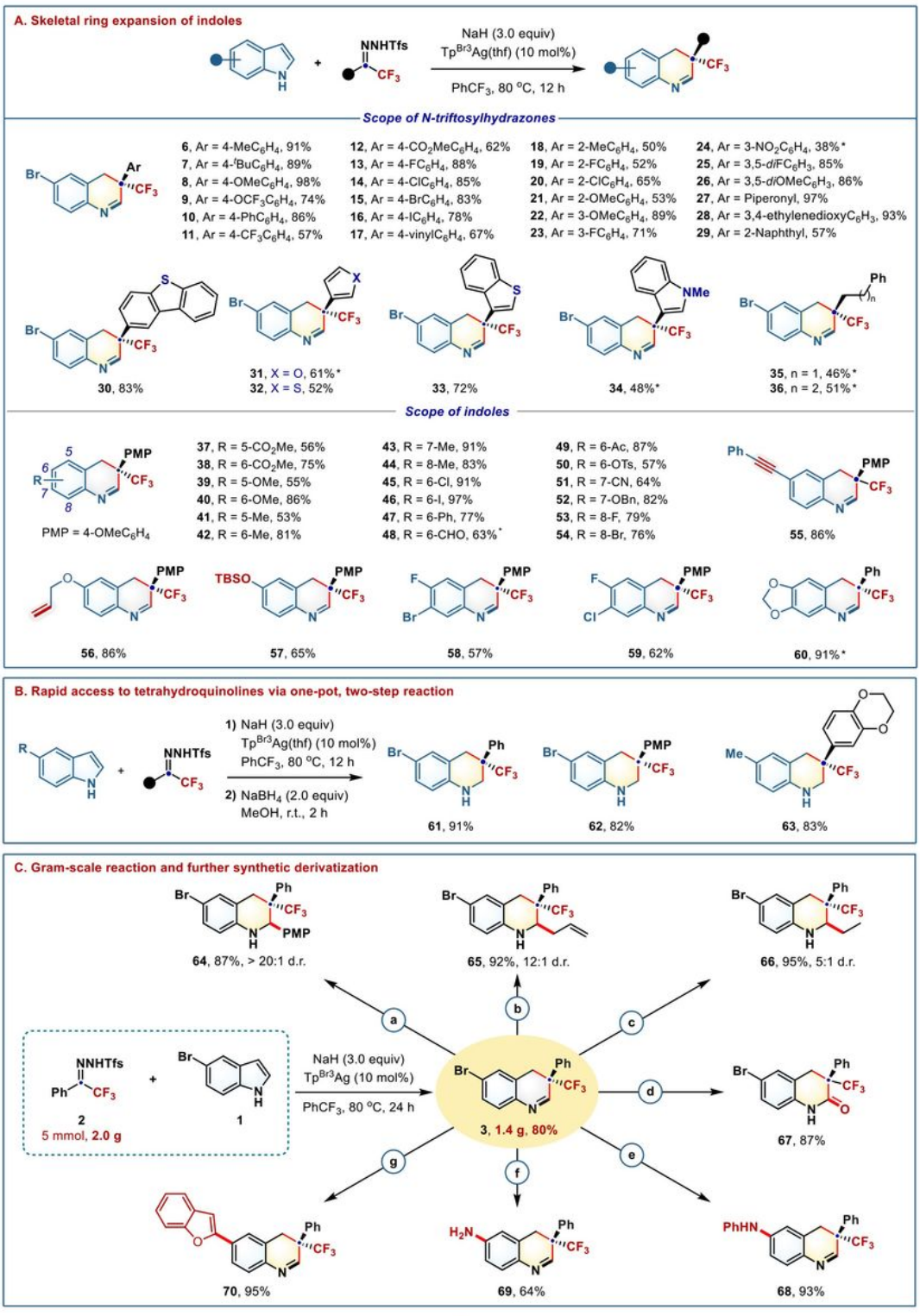

Figure 3

Skeletal editing of indoles with fluoroalkyl *N*-triftosylhydrazones. (**A**) Scope of carbon-atom insertion into indole skeletons. (**B**) Two-step, one-pot process to access tetrahydroquinolines. (**C**) Gram-scale reaction and further synthetic derivatization. Yields are given for isolated products. *1 mol% $Rh_2(esp)_2$ was used as catalyst instead of $Tp^{Br3}Ag(thf)$.

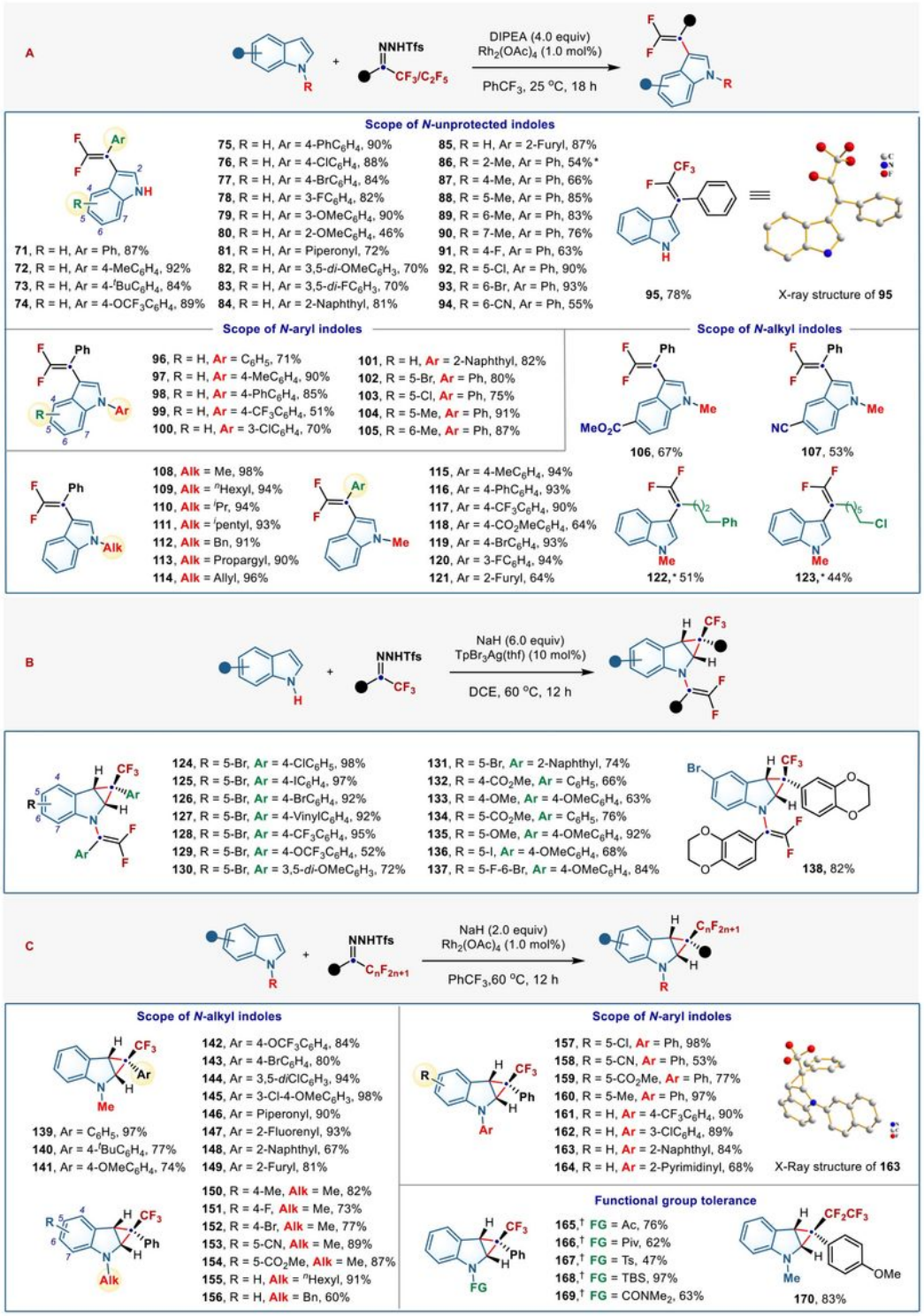

Figure 4

Peripheral editing of indoles with fluoroalkyl *N*-triftosylhydrazones. (A) Scope of C–H *gem*-difluoroolefination. **(B)** Scope of tandem cyclopropanation and N–H *gem*-difluoroolefination. **(C)** Scope of dearomative cyclopropanation. *Reactions were performed at 40 °C. †10 mol% $Tp^{Br3}Ag(thf)$ was used as catalyst.

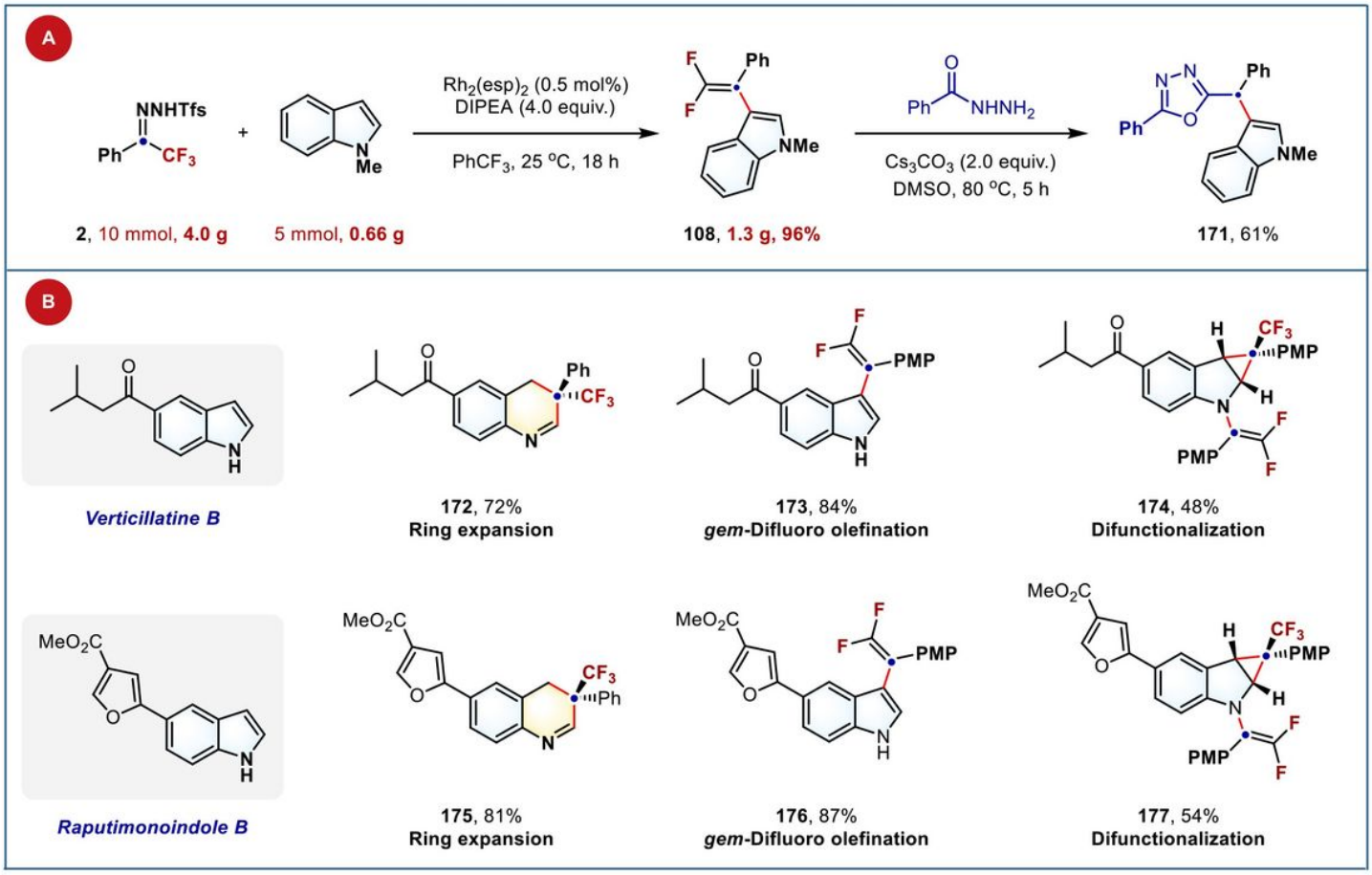

Figure 5

(A) Gram-scale reaction and synthetic derivatization. **(B)** Late-stage editing of natural products.

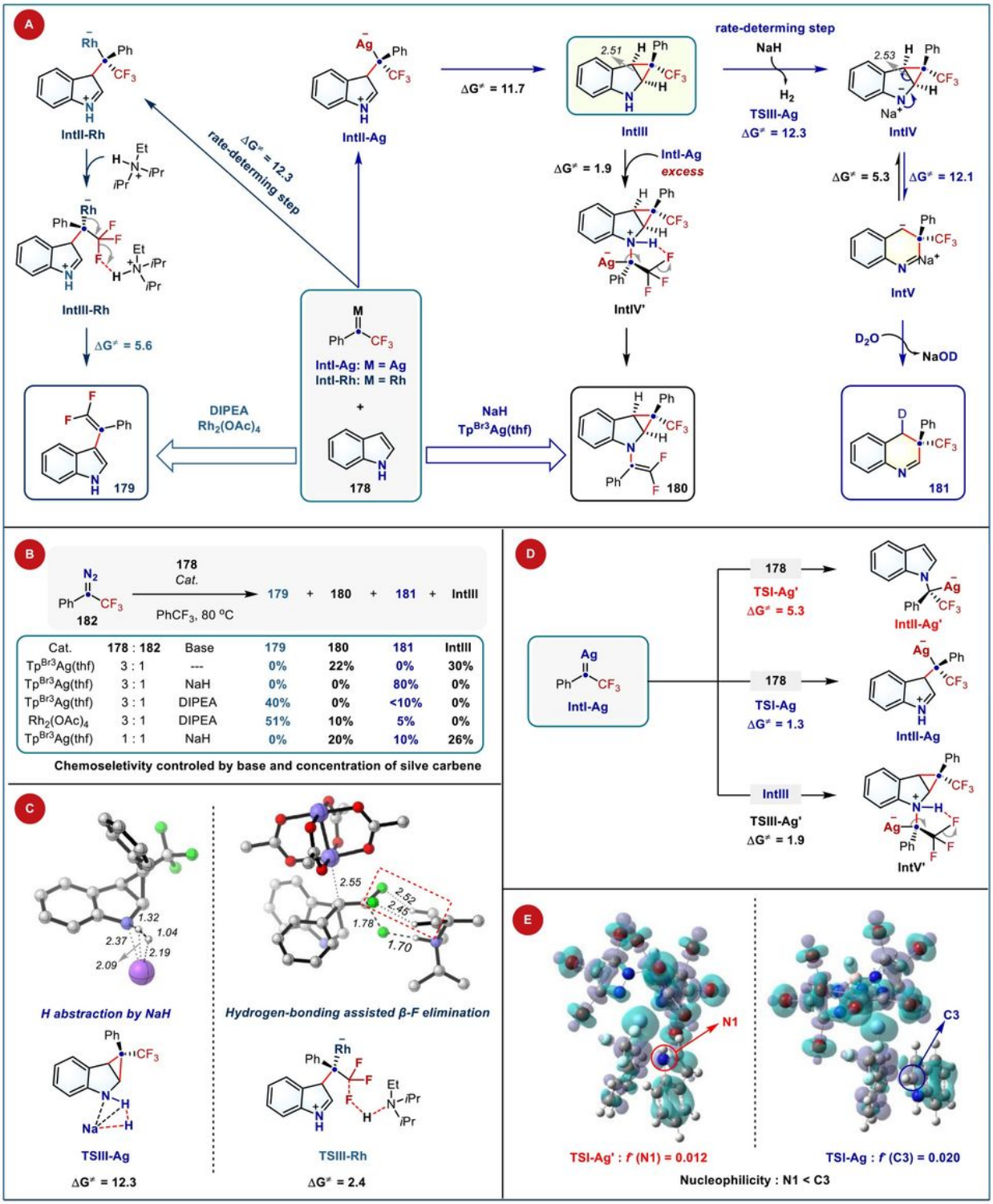

Figure 6

Mechanistic investigations. (**A**) Proposed mechanisms. $\Delta G^{\neq}$, Gibbs energy barrier. All barriers are given in kcal mol^{-1}. Distances in angstroms. (**B**) Control experiments using phenyl trifluoromethyldiazomethane as a carbene precursor. (**C**) DFT-optimized lowest-energy transition structures for H abstraction by NaH leading to carbon-atom-insertion product **181** and hydrogen-bonding-assisted β-F elimination leading to *gem*-difluoroolefination product **179**. (D) The relative reactivity of silver carbene **IntI-Ag** towards C3–H and

N1−H of indole and **IntIII**. (E) Fukui function analysis for **TSI-Ag** and **TSI-Ag'**. Orbital-weighted *f*− (purple) represents electrophilicity and orbital-weighted *f*+ (green) represents nucleophilicity.

Supplementary Files

This is a list of supplementary files associated with this preprint. Click to download.

- CIFFolder.zip
- SupplementaryInformation1.pdf
- SupplementaryInformation1.docx